Ambidextrous bend patterns in free-standing polar smectic-CP_F films

Alexey Eremin,[1] Alexandru Nemeş,[1] Ralf Stannarius,[1] and Wolfgang Weissflog[2]
[1]*Otto-von-Guericke-Universität Magdeburg, IEP, Department of Nonlinear Phenomena, Universitätsplatz 2, D-39016 Magdeburg, Germany*
[2]*Martin-Luther-Universität Halle, Institut für Physikalische Chemie, Mühlpforte 1, 06108 Halle (Saale), Germany*
(Received 17 April 2008; revised manuscript received 6 October 2008; published 12 December 2008)

We report an unusual behavior of a ferroelectric smectic-CP_F film formed by bent-shaped molecules. The ground state of the *c*-director in such film is not uniform but forms a striped pattern with alternating bend deformation. We found that the sense of the alternating bend is not related to an alternating handedness defined by the mutual orientation of the tilt (*c* director) and the bow (*p* director) of the molecules. Despite its similarity to a previously described twist-bend instability [J. Pang and N. A. Clark, Phys. Rev. Lett. **73**, 2332 (1994)], this pattern cannot be explained in terms of spontaneous chiral symmetry breaking with continuous variation of the chirality order parameter, since the synclinic order of the polar molecules predefines the chirality of the film. We discuss possible models describing the spontaneous formation of an ambidextrous bend pattern of the *c* director.

DOI: 10.1103/PhysRevE.78.061705 PACS number(s): 61.30.Hn, 64.70.mj

INTRODUCTION

Freely suspended smectic films present an excellent system to study mesophase behavior and phase transitions in quasi-two dimensions [1,2]. In a smectic-CP_F (Sm-*C*) phase, the projection of the director **n** on the smectic layer defines a vector order parameter $\mathbf{c}(x,y)$ [1,3]. Thus the energy of the elastic deformations is given by the derivatives of the director in a similar way as it is in nematics [4]. The transitions between different phases can be described in the frame of the *XY* model [5,6]. Additional symmetries and couplings of the order parameter to the external field or the geometric constraints given by the boundary of the film may considerably complicate the system. The competition between different interactions often favours incompatible ground states and leads to a frustration. In this instance, thin films of ferroelectric liquid crystals are of particular interest since their study could shed light on the role of polarity and chirality in the pattern formation.

Periodically disturbed patterns of the order parameter and arrays of defects have been extensively studied in freely suspended smectic films and Langmuir monolayers [7,8]. Symmetry breaking, either chiral or asymmetry of the interfaces, is one of the ingredients required for the formation of periodic patterns in the films. Stripes having one sign of bend have been found in films of chiral compounds [9]. In achiral materials, the chiral symmetry can be broken leading to formation of patterns with alternating sign of the bend and therefore with alternating chirality [9–12]. Except for patterns with continuous variation of $\mathbf{c}(x,y)$, organized defect structures have been observed. Point vortices, as well as lines (or strings) also typical for other two-dimensional (2D) *XY* systems have been reported in the literature [13].

In our paper, we study freely suspended films of bent-shaped mesogens in the ferroelectric Sm-CP_F phase. Periodic distortions of the director field in the form of stripes with alternating bend of $\mathbf{c}(x,y)$, first reported in such films in our previous paper [14], are very similar to the twist-bend instability patterns reported in [10]. However, the mechanism of chiral symmetry breaking in a calamitic compound shown in [10] is very different from the one described here. Despite that the bent-shaped mesogens themselves are achiral, the smectic structure in the free films of latter materials is chiral [15]. The chiral order in a single layer can be described by an order parameter $q=([\mathbf{c}\times\mathbf{k}]\cdot\mathbf{p})$, where **k** is the layer normal and **p** is a polar director along the direction of the molecular bow. In the case of a synclinic arrangement of the molecules in adjacent layers, the whole film becomes homochiral. Contrary to the Sm-C^* phase, the macroscopic polarization appears in a self-consistent way and is not a secondary order parameter any more, thus the Sm-*CP* phase is a proper ferroelectric. As a result, different mechanisms can contribute to the switching process in the "banana-phase," and the chirality *q* can also be varied by external fields. In freely suspended films, a change of sign of *q* would require either formation of defect lines where **c** or **p** are discontinuous or continuous variation of this order parameters across domain walls. In our experiments, we observed that the stripes with opposite bend have the same sign of the chiral parameter *q*. This indicates a mechanism for formation of the periodic pattern in Sm-CP_F films qualitatively different from that described in [10]. In a previous report [14], we have introduced a principal characterization of the novel type of periodic pattern, and proposed an elastic model based on the assumption of a negative bend elastic constant. Here, we discuss details of the pattern formation process in different topologies, we characterize the behavior of the pattern in electric fields in order to determine the polarization direction and sign of the chiral parameter, and we discuss the possible physical background of an effective negative bend constant.

EXPERIMENT

The structural formula of the bent-shaped mesogen is given in Fig. 1 [16,17]. Two monotropic mesophases have been observed on cooling of the isotropic liquid in bulk. The high temperature nematic phase is separated by a first-order phase transition from a Sm-CP_F phase [16,17]:

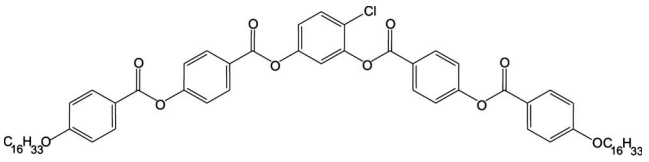

FIG. 1. Chemical formula of the investigated compound 16.

$$\text{crystal} \underset{99°C}{\leftrightarrow} (\text{Sm}-CP_F \underset{88°C}{\leftrightarrow} N) \underset{92°}{\leftrightarrow} \text{isotropic}.$$
$$[34.8\ \text{kJ/mol}] \qquad [3.5\ \text{kJ/mol}] \quad [12\ \text{kJ/mol}]$$

The Sm-CP_F phase is a tilted smectic phase with a very large tilt angle, reaching 50° (assessed from the layer spacing measurements), and without in-plane order.

Free-standing films have been drawn over a custom-made rectangular glass frame with a 10 mm × 3 mm slit and two brass electrodes. The frame has been mounted into a Linkam LTS 350 heating stage. The temperature controller provided an accuracy of 0.1 K. Optical observations have been made with a polarizing microscope AxioImager Pol (Carl Zeiss GmbH) equipped with a high-resolution cooled charge-coupled device (CCD) camera AxioCam HR (Carl Zeiss GmbH). We carried out the observations in reflected light between crossed polarizers as well as between slightly decrossed polarizers. Under slightly decrossed polarizers, the light intensity dependence on the azimuthal angle φ of the *c* director with respect to the *x* axis can be expressed in first approximation in the form

$$I(\varphi) \approx I_0 + I_1 \sin 2(\varphi - \alpha_p - \delta/2),$$

provided the retardation of the thin film is sufficiently small; α_p is the polarizer angle and δ is the mismatch angle of the analyzer from the crossed position (in our experiments $\delta = 10°$, the position of polarizers is given in Fig. 2). At sufficiently large mismatch angles (a few degrees), the intensity profile $I(\varphi)$ has only two maxima (in contrast to four maxima at crossed polarizers) and the angle φ modulo π can be deduced from intensity measurements. In our experiments we mapped the director field by marking the positions of the intensity maxima at a given orientation of the polarizers. By rotating the whole film in this geometry and marking the reflectivity extrema at each step, we obtain a reliable map of the director field without the need to employ an explicit expression for $\varphi(I)$. The determination of the molecular tilt direction has been performed at inclined incidence in the transmission mode of the microscope. In order to improve the brightness of the microscopic patterns (especially at crossed polarizers) we used an HBO 100 illumination house with a 100-W mercury-vapor lamp. Measurements of the film thickness have been done by analysis of the apparent interference color in reflection. Thus combining both depolarized reflected light microscopy (DRLM) and transmission

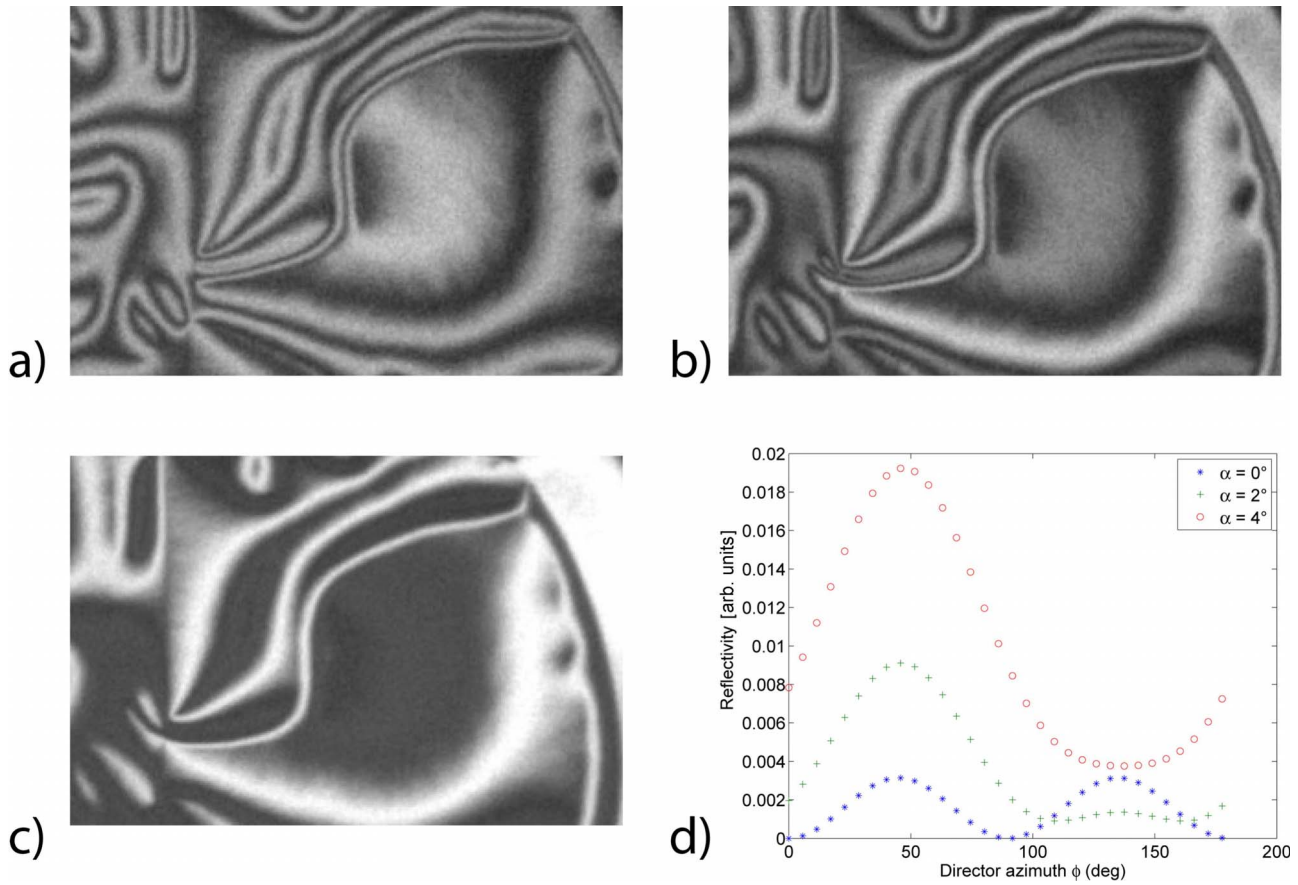

FIG. 2. (Color online) A fragment of the film imaged between (a) crossed ($\delta = 0°$) (b) uncrossed polarizers with the mismatch angle of $\delta = 2°$ (c) $\delta = 6°$ (d) computed reflection curves for selected mismatch angles α.

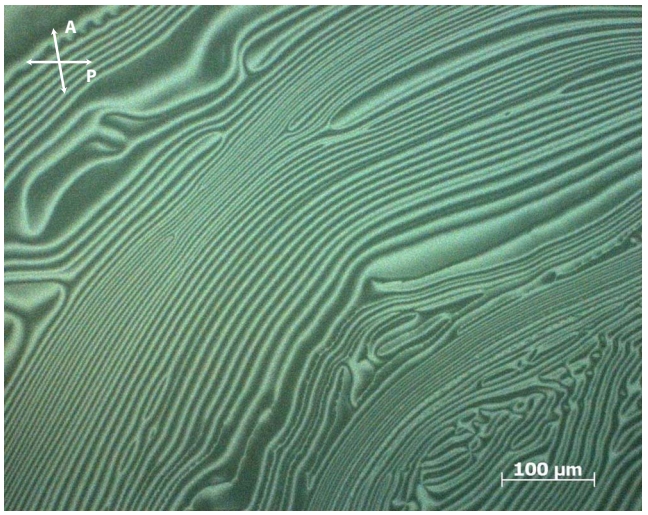

FIG. 3. (Color online) Ripple structures in a free-standing film at $T=87$ °C between slightly (10°) uncrossed polarizers.

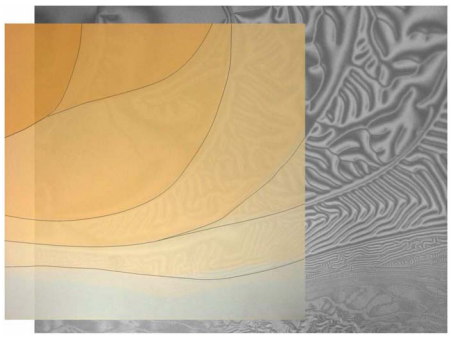

FIG. 4. (Color online) Texture of ripples between slightly decrossed polarizers and a superimposed image of layer steps observed in ($T=88$ °C). The thickness ranges from approximately 22 molecular layers (upper left corner) to 15 layers (at the bottom). In this image, the borders of the layer steps are emphasized by black lines for a better visibility. In thinner film the ripples become more densely packed. However, this state is transient and with time the density of ripples equalizes.

polarized light microscopy at inclined incidence, we can completely map the c director. The direction of spontaneous polarization (p director) is determined through in-plane switching as described below. Two electrodes attached to the glass frame allowed application of electric fields in the plane parallel to the film. The voltage was provided by an arbitrary wave generator TGA 1241 (TTi).

RESULTS

In our previous paper we have already described the behavior of the Sm-CP_F phase (designated as Sm-X) in sandwich cells [16,17]. We observed ferroelectric switching which was stronger pronounced at lower temperatures. Perhaps the most extraordinary feature of this material is that at high voltages (and low temperature) birefringent fan-shaped textures could be transformed into an isotropic texture with chiral domains [16]. The handedness of those domains could be switched with sufficiently strong electric field. Despite that there are some models involving "dark conglomerate phase" and spongelike structures [18,19], the structure of this chiral isotropic state remains still unclear.

Freely suspended films have been prepared at the temperature 89–90 °C. The transition into the nematic phase turned out to be several degrees higher in film geometry. In most experiments, we worked with films of thickness about 60–140 nm. A schlieren texture can be easily identified in polarized light pointing to a tilted arrangement of the molecules within the smectic plane. The texture has a quite high contrast which can be attributed to an unusually high tilt angle (up to 50°) reported in our previous studies [14]. A director reorientation by the electric field has been observed in films of the Sm-CP_F phase indicating a polar in-plane order.

A spontaneous regular stripe pattern with a period of the order of 5 μm attracts particular attention. The stripes are formed by lines (or strings) which cover the whole area of a freshly prepared film (Fig. 3). On heating up into the nematic phase, convective flows in the free-standing film deform and smear the regular stripe pattern. The first-order Sm-CP_F–N transition is manifested by a moving boundary separating the two coexisting mesophases in a temperature gradient and thickening of the film. This convective motion occurs due to the difference of the surface tension between the two phases. We attribute its origin to a slight temperature gradient in the film and mechanism similar to that described by Godfrey and van Winkle [20]. On the Sm-CP_F side the schlieren textures remain low mobile; at the same time, the nematic side looks very turbulent. The stability of the nematic films is probably caused by a surface-induced smectic ordering.

Shortly after the film is prepared, before a steady texture is reached, the density of the stripes in the Sm-CP_F phase seems to depend on the film thickness (Fig. 4); however, the apparent variation of the stripe density can arise from the difference in relaxation dynamics during the stripe growth. Since the director is anchored at the layer steps, the strings cannot penetrate across the boundaries and the pattern coarsening in different islands occurs independently. After several hours, the film contains stripes with different wavelengths independent of the film thickness. The ultimate pattern con-

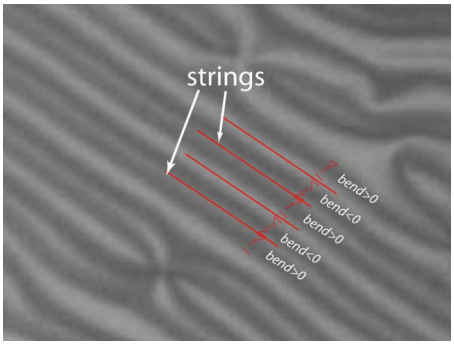

FIG. 5. (Color online) Ultimate pattern consisting of stripes with alternating bend separated by $\Omega=0$ strings. Both c and p directors remain continuous as one crosses the string so that the chiral parameter q does not change its sign (see the text).

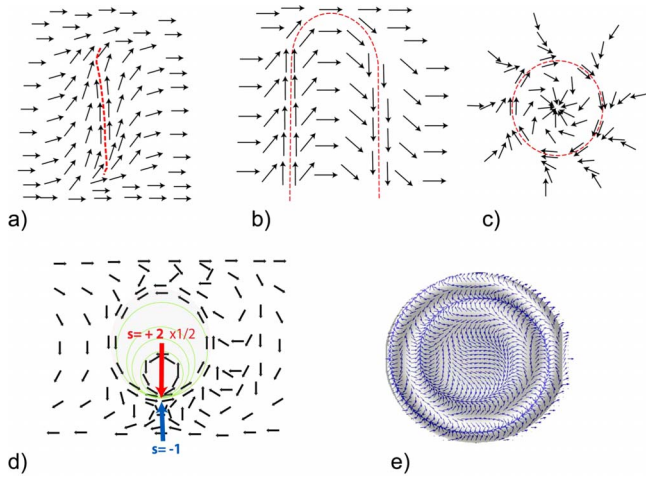

FIG. 6. (Color online) Different morphologies observed in the film: (a) single string, (b) pin, (c) spiral with an $s=+1$ vortex in the center, (d) boojum, (e) target pattern. The arrows show the c director.

sists of stripes with alternating bend (Fig. 5). The stripes do not disappear on heating before the transition into the nematic phase takes place.

On cooling the striped pattern becomes metastable and disappears after approximately 2 days at $T=89$ °C. At lower temperatures the film crystallizes before the pattern disappears. The transition from the nonmodulated into a modulated state can be achieved by heating the film. In this case, however, the temperature range of the modulated state is confined to approximately 2 K before the transition into the nematic phase takes place.

Morphologies of stripes

In the freshly prepared films, the director field is strongly inhomogeneous. Stripes, either disordered or organized into a periodic pattern, cover the whole area of the film. Occasionally, a freshly drawn film has large areas without stripes. In those cases the stripes nucleate and fill up the film completely within $\frac{1}{2}-1$ h. We could distinguish several types of morphologies (Fig. 6): The first type is a single line which nucleates in a homogeneously oriented director filed. The director field exhibits a bend deformation in the vicinity of the line. Detailed microscopy observations have shown that upon crossing the line both components of **c** (tangential and normal) remain continuous and the sense of bend changes [Figure 7 and 6(a)]. Additionally, as it will be shown below, the polar director **p** is perpendicular to the line and continuous. Those strings are remarkably similar to the lines designated as $\Omega=0$ strings (Ω is topological strength) in Ref. [13]. It is important to emphasize that our strings are not defects since the field of the director is continuous. The strings are distinguished rather by an apparent spatial discontinuity of the derivative of **c**, which makes them optically visible (it should be noted that in the experiment, a discontinuous behavior cannot be distinguished from a strong continuous inflection of the bend deformation). Such single lines can be found only in freshly drawn films. With time, the lines grow and buckle resulting in a "hairpin" or "finger" morphology Figs. 8, 9, and 6(b). This is the most common structure we observed. Such fingers grow and buckle resulting in an intricate labyrinth pattern. Within each finger, the c director makes a π turn from one line to the other hence creating a pattern with a alternating bend of the c director (Fig. 5). The third morphology "closed loop," could be observed only occasionally [Fig. 6(c)]. Closed loops consist of a vortex of topological strength $s=+1$ enclosed by a string. The director is tangential to the string and the bend deformation is of opposite sense in the inner and outer domains delimited by the loop. Another striking feature of the pattern formation is the occurrence of boojum textures in loops [Figs. 10 and 6(d)]. Such circular-shape loops contain one-half of an $s=+2$ vortex pinned to the loop from the inner side (yielding the overall topological strength +1). On the outer side of the

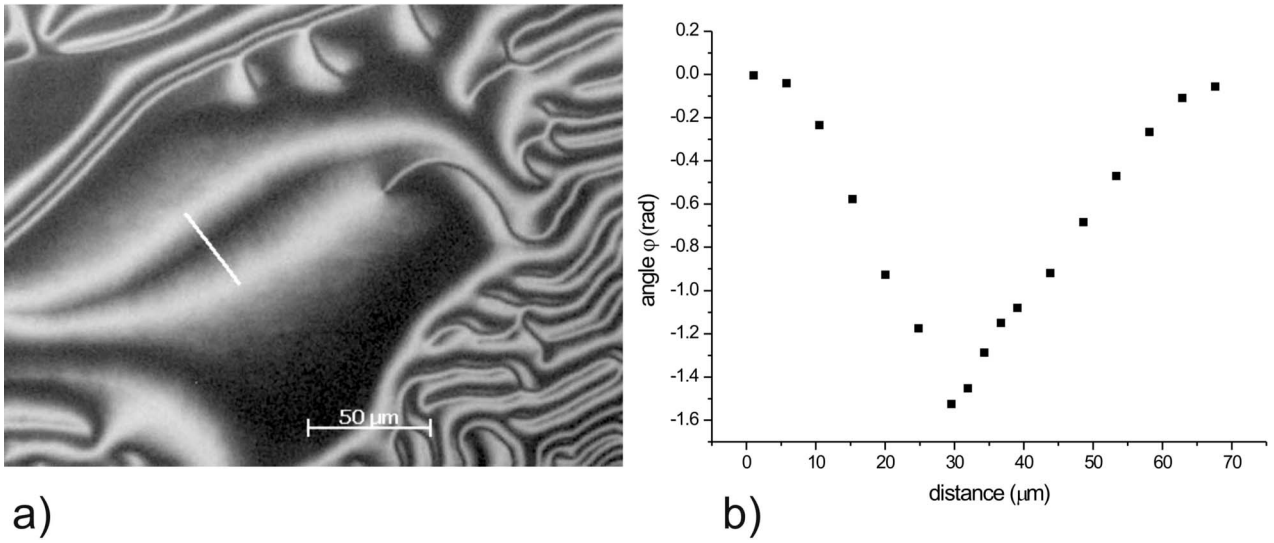

FIG. 7. (a) (a single string dividing two domains with opposite bend; (b) azimuthal angle profile along the section given in (a) and the c director along the section line.

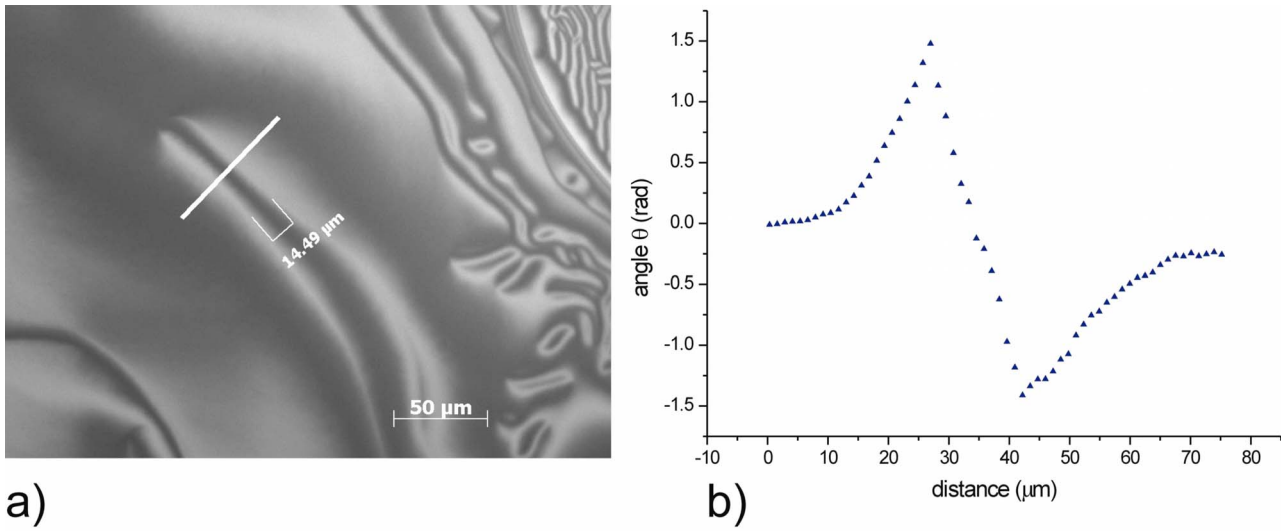

FIG. 8. (Color online) (a) Finger consisting of a U-shape single line; (b) azimuth-angle profile and director field along the section given in (a).

loop there is a structure with the appearance of a defect of strength −1. Actually, the resolution of the microscope is not sufficient to distinguish unambiguously whether there is a pair of defects or two strong deformations of the director field with a narrow short wall in between. The whole structure has a net topological strength 0, which is consistent with its spontaneous formation in a homogeneous director field. Boojum loops grow and deform into prolonged batonnets [Figure 10(b)].

On heating, the formation of modulated pattern in homogeneous regions is marked by periodic deformation of the director field (Fig. 11) and nucleation of single lines which tend to take up a finger shape or in the form of growing "hairpins" (Fig. 12). The hairpins themselves buckle and form fingerlike structures with a bend. Another interesting phenomena observed at the onset of transition from a homogeneous into the modulated state is a formation of target patterns [Figs. 6(e) and 11]. Such patterns have a nearly cylindrical symmetry and the c director makes several rotations as one goes from the center of the pattern to the periphery. The pattern optically consists of several concentric rings where bend and splay regions of **c** alternate forming a target or spiral-like structure. Despite the fact that the target patterns can result from convective flows in the film during the transition, and have been observed in many other materials, it is remarkable that the patterns in our material remain stable at higher temperatures and can be unwound by lowering temperature upon the transition into the homogeneous state.

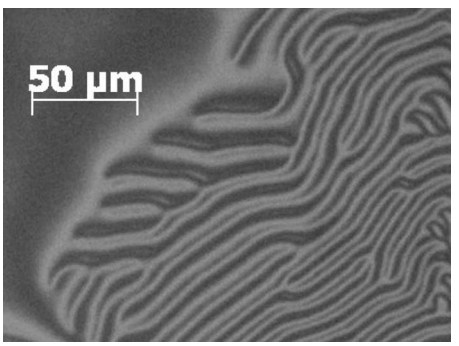

FIG. 9. Branching of hairpins.

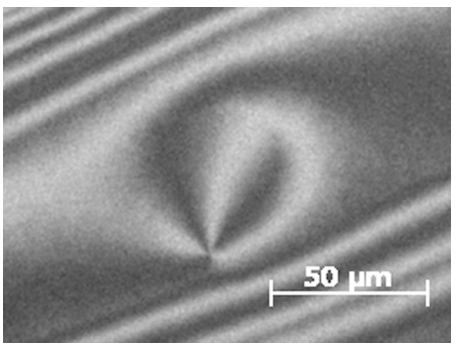

(a)

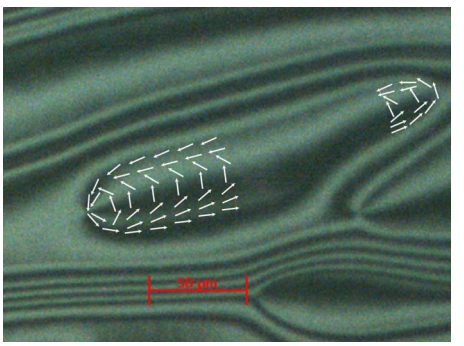

(b)

FIG. 10. (Color online) Boojum textures with $s=+2$ vortex (a) and growth of fingers from the loops (b).

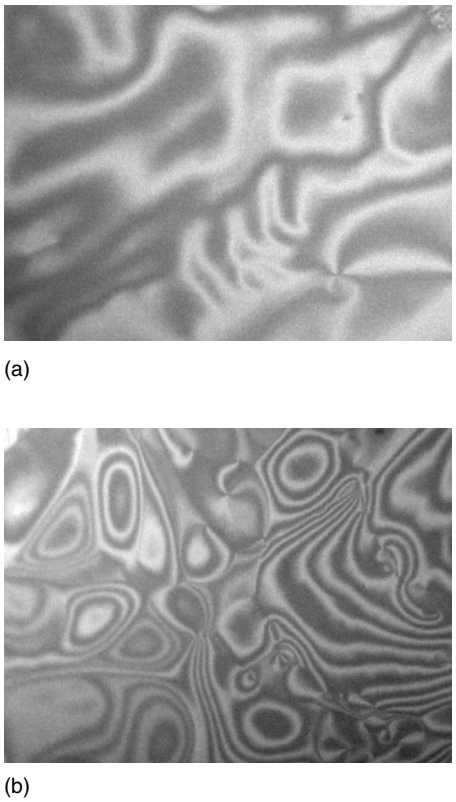

FIG. 11. (a) Continuous deformation of the director field at the instability onset on heating; (b) spontaneously forming target patterns ($T=90\ ^\circ$C).

Behavior in electric field

To determine the direction of the spontaneous polarization in the film, we studied the director reorientation in an electric field. An applied DC electric field in the film plane aligns the *c* director in a direction perpendicular to the electric field, which means that $\mathbf{p} \perp \mathbf{c}$. No odd-even effect of the number of layers in the reorientation behavior has been observed, confirming a ferroelectric structure of the film. For fragments of a single string, the extinction brushes move in opposite directions on both sides on application of a field. Application of a field of one polarity along the line decreases the bend deformation aligning the *p* director parallel to the field. The field of opposite direction produces a reverse effect and, at higher voltages, it turns the string perpendicular to the field. Fingers aligned parallel to the electric field shrink at one polarity and dilate at the other. Switching is possible only when the density of the strings is quite low (in a freshly drawn film). An example of field-induced reorientation of the *c* director is given for a fragment containing four parallel strings in Fig. 13. These findings indicate that **p** remains continuous upon crossing the strings. When the film is completely covered by the labyrinth the reorientation cannot be observed since it would require very strong deformations of the *c* director. The period of stripes varies significantly from 20 μm to a submicrometer size. It does not depend on film thickness or temperature: areas with different periodicities can be encountered in a film of constant thickness. Since the relaxation into equilibrium is very slow, it is hard to distinguish a frustrated pattern from an asymptotically reached equilibrium state. An apparent tendency for the fine structures to be formed at lower thickness can be observed only in freshly drawn films and can be attributed to a slower kinetics of stripe formation in thicker films. In some areas, the stripe period becomes smaller and reaches the resolution limit of the microscope. This local quasiperiodicity enforces a 2D focal-conic-like texture on larger scales which can be seen because of the anisotropy in the local mean orientation of **c** relative to the stripes. In thick films (>350 nm), the string pattern does not appear at all, instead, one observes a kind of broken schlieren texture.

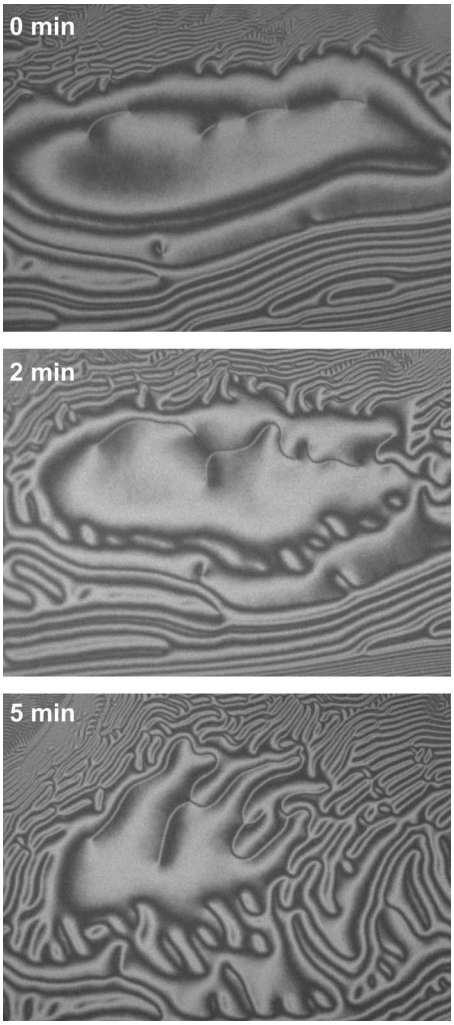

FIG. 12. Nucleation and growth of pins (double strings) $T=91\ ^\circ$C from π walls; the width of the line is 2.6 ± 0.5 μm.

Broken schlieren texture

Another interesting pattern has been observed in thicker films (above 100 nm) near the meniscus: the schlieren texture becomes broken in small rectangular domains or, sometimes, ribbons with a size of about 2–20 μm. The texture becomes similar to a pattern of a parquet floor. The director is homogeneous within each domain, and the orientation of the domains slightly changes in order to follow the director

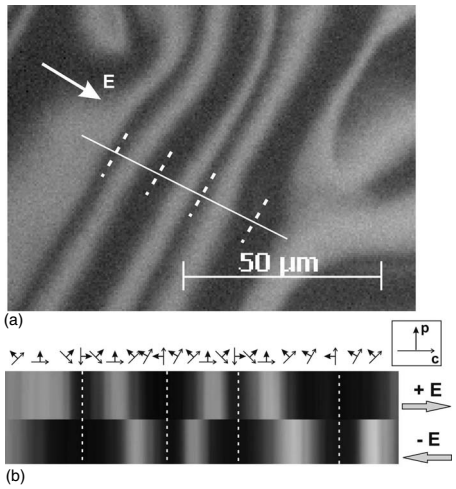

FIG. 13. Behavior of the director field between the strings: (a) an image with four strings (marked by dashed lines) in the electric field 40 V/mm; (b) sections along the profile given in (a) for the states at +40 V/mm (above) and −40 V/mm (below). The images show that the p director is continuous across the strings.

in the preceding schlieren texture. This texture is particularly well pronounced if there is a big droplet in the film with the thickness up to 1 μm. The rectangular domains inlay the droplet so that the c director is on average tangential to the perimeter (Fig. 14). It is not clear what the reason for existence of droplets in a Sm-CP_F film is. One explanation could be that they appear at high temperature when the transition into the nematic phase takes place. During this transition, thickening of the film occurs, and big droplets start to form. On cooling, however, the material flows back into the meniscus and, at the same time, the texture in the droplets turns from schlieren into the broken schlieren. This ordering transition then hampers the flow of the material from the droplet leaving them stable at lower temperatures, sometimes creating lattices of ordered droplets such as in other liquid-crystal films [21].

DISCUSSION

First, it must be pointed out that despite the fact that freely suspended Sm-C-like films are described by a two-dimensional director $\mathbf{c}$, they are actually quasi-two-dimensional. This means that the c director follows particular transformation rules (see, for instance, Ref. [9]). As a result, the c director bend deformations of opposite sense are mirror symmetric, they are, chiral. In the following we will restrict our discussion to a two-dimensional director structure. Any deformations of the director field along the layer normal will be neglected. As a matter of fact, presence of a considerable short-wave helical twist along the layer normal in 100–200 nm films seems to be improbable and energetically too costly. All deformations discussed here are basically long wave (100 nm–1 μm). It should be stressed, however, that our experimental data can not exclude the presence of a small helical twist in the z direction, which should be accounted for in a more general 3D model.

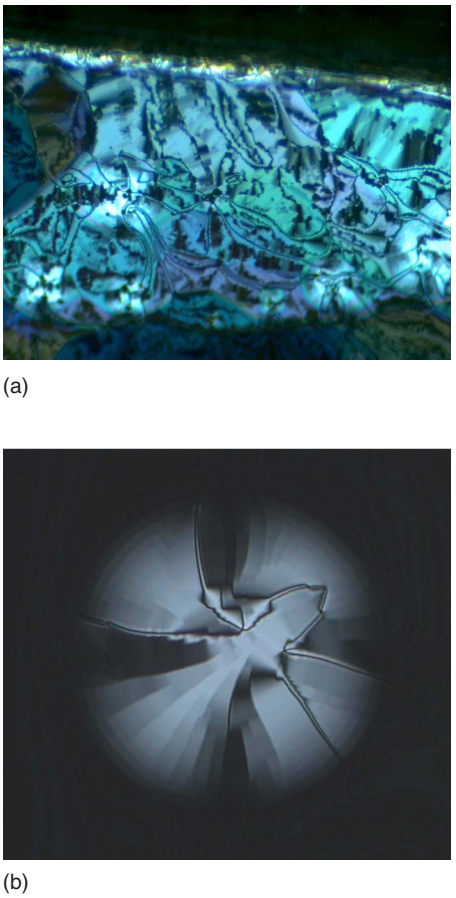

FIG. 14. (Color online) Broken schlieren texture near the meniscus (a) and in a droplet on the film surface (b).

Before turning to a discussion of the mechanisms contributing to this particular pattern formation, let us outline the main experimental findings: we have a Sm-CP_F phase in a homochiral state, which is defined by the mutual orientations of the c and p directors. The final state consists of stripes with alternating c director bend. There is no preferred handedness of the stripes, i.e., they are ambidextrous. Both senses of bend are equally preferable.

Periodic bend deformations of the c director and formation of strings in both chiral and achiral smectic phases are not new [10,11]. In freely suspended Sm-C films with equivalent interfaces, the bulk free energy up to square order in c director gradients consists of splay and bend terms

$$F_{\text{bulk}} = \frac{1}{2}\int d^2x[K_s(\nabla \cdot \hat{\mathbf{c}})^2 + K_b(\nabla \times \hat{\mathbf{c}})^2] \qquad (1)$$

where K_s and $K_b > 0$ are nematiclike splay and bend elastic constants, respectively, and $\hat{\mathbf{c}}$ is a unit vector along $\mathbf{c}$. The full energy will additionally contain surface terms and the energy of the defects in the film. Destabilization of homogeneously oriented director field can occur as a result of chirality of the phase [9,12], director coupling to the undulation of the smectic layers [8] and negativity of the bend elastic constant [1,22]. In order to describe periodic structures, one should also consider higher-order terms in gradients and al-

low variation in the magnitude of **c**. A model for spontaneous breaking of achiral symmetry and formation of periodic stripe pattern has been proposed by Selinger *et al.* (SWBK model) [12]. This model predicts a continuous breaking of achiral symmetry described by a pseudoscalar order parameter ψ, which couples to the bend of the $\hat{\mathbf{c}}$ director through a term $\lambda\psi\nabla\times\hat{\mathbf{c}}$. Then the free energy can be expressed by

$$F_{bulk}=\frac{1}{2}\int d^2x\left(\left[\kappa(\nabla\psi)^2+t\psi^2+\frac{1}{2}u\psi^4\right]+K_s(\nabla\cdot\hat{\mathbf{c}})^2+K_b(\nabla\times\hat{\mathbf{c}})^2-\lambda\psi\nabla\times\hat{\mathbf{c}}\right). \quad (2)$$

The terms in square brackets are the Landau expansion of free energy in powers of the order parameter ψ. The coefficient t passes through 0 as a function of temperature. Apart from uniform nonchiral and chiral phases, this model displays several other phases with periodic sinusoidal stripes, soliton structures, and square lattices. This model has been successfully applied to describe patterns in Langmuir films and achiral Sm-*C* phases. A slightly modified SWBK model has been employed to describe a twist instability reported by Pang *et al.* [10]. This instability occurs as a result of a strong difference of opposing perfluoro and perhydro alkyl tails of the investigated compound. Resulting polar ordered layers favour a spontaneous twist of the **n** director which, in return, gives rise to the bend of the **c** director. Thus initially achiral films display a chiral symmetry breaking in the form of periodically changing bend deformations across the film.

The soliton regime occurs immediately when the film is drawn in the Sm-CP_F phase. It seems that the SWBK model can be applied to our case as well. However, there are significant distinctions too. In our case, the film is chiral already in an undistorted state. The synclinic ferroelectric structure of the layers defines the handedness of chirality [23]. Moreover, the large tilt angle of the molecules points to a strong chirality. On the other hand, developed patterns consist of stripes with alternating bend of **c**. At the same time, the widths of the stripes with opposite bend are the same. This means that the pattern does not prefer any particular sign of the bend, i.e., it is ambidextrous. Enclosed circular and batonetlike loops developing from boojums textures can be stable if the structure with spontaneous bend is preferred like in chiral films [12]. A model different from SWBK can be considered to account for ambidextrous bend in which the effective bend elastic constant becomes negative. Within the continuum elastic theory we consider the free energy in the form given in Eq. (1). In the case when $K_b<0$ Eq. (1) should include higher order terms in gradients of **c**. We will restrict our simplified model to the inclusion of a fourth power term of $\nabla_z\times\hat{\mathbf{c}}$ in the free energy,

$$f=\frac{K_s}{2}(\nabla\cdot\hat{\mathbf{c}})^2+\frac{K_b}{2}(\nabla\times\hat{\mathbf{c}})^2+\alpha(\nabla\times\hat{\mathbf{c}})+\frac{K_{b4}}{4}(\nabla\times\hat{\mathbf{c}})^4, \quad (3)$$

where $K_s>0$ is the splay elastic constant, K_b is the effective bend elastic constant, α is the pseudoscalar coefficient accounting for spontaneous bend in a chiral film, K_{b4} 0 is the elastic constant at the fourth-order bend term required for stability of the ground state. The length- scale in this system is given by $R_0=\sqrt{K_{b4}/|K_b|}$. This *ad hoc* description is certainly oversimplified and incomplete: other terms in the expansion which may have comparable amplitudes have been neglected. On the other hand, as it is shown below, the model qualitatively describes the experimental observations. Restricting the description to a one-dimensional case, we express the **c** director through the phase angle $\varphi(x)$: $\hat{\mathbf{c}}(x)=(\cos(\varphi),\sin(\varphi))$. In this case the free-energy density Eq. (2) is given by

$$f=\frac{K_s}{2}\sin^2\varphi\cdot\varphi'^2+\frac{K_b}{2}\cos^2\varphi\cdot\varphi'^2+\alpha\cos\varphi\cdot\varphi'+\frac{K_{b4}}{4}\cos^4\varphi\cdot\varphi'^4 \quad (4)$$

or dividing by $K_s/2$

$$\tilde{f}=\sin^2\varphi\cdot\varphi'^2-\varepsilon\cos^2\varphi\cdot\varphi'^2+\gamma\cos\varphi\cdot\varphi'+\beta\cos^4\varphi\cdot\varphi'^4, \quad (5)$$

where $\varepsilon=-K_b/K_s$, $\gamma=2\alpha/K_s$, and $\beta=K_{b4}/2K_s$.

The first integral of the Euler-Lagrange equation yields $f-\varphi'\cdot\partial f/\partial\varphi'=\text{const}$, i.e.,

$$-\sin^2\varphi\cdot\varphi'^2+\varepsilon\cos^2\varphi\cdot\varphi'^2-3\beta\cos^4\varphi\cdot\varphi'^4=\text{const}. \quad (6)$$

Looking for solutions continuous in φ and φ' which minimize the free energy Eq. (6), we set the constant to zero (since φ' is periodic and changes its sign) and arrive at the expression

$$\sin^2\varphi\cdot\varphi'^2-\varepsilon\cos^2\varphi\cdot\varphi'^2+3\beta\cos^4\varphi\cdot\varphi'^4=0. \quad (7)$$

Equation (7) has a trivial solution $\varphi(x)\equiv 0$. Two other specific solutions can be reduced to the quadrature

$$\varphi'=\pm\sqrt{\frac{-\sin^2\varphi+\varepsilon\cos^2\varphi}{3\beta\cos^4\varphi}}. \quad (8)$$

Real solutions of Eq. (7) are periodic in φ, they exist only for $\varepsilon>0$ (opposite signs of splay and bend constants), and they are confined to the segment $(-\varphi_{\max},\varphi_{\max})$, where $\varphi_{\max}=\arctan\sqrt{\varepsilon}=\arctan\sqrt{-K_b/K_s}$. Experimentally, the angle $\varphi_{\max}$ is rather close to $\pm\pi/2$. A solution that fills up the whole space can be constructed by combining the two branches of the specific solutions of Eq. (7). Plots of $\varphi(x)$ for selected parameters are shown in Figs. 15 and 16. These inhomogeneous solutions have a lower free energy than the homogeneous state: the elastic energy of the nondeformed state is equal to zero. It is straightforward to show that in the deformed state, the local energy density is

$$\hat{f}=2f/K_s=-\frac{1}{9}\frac{(\sin^2\varphi-\varepsilon\cos^2\varphi)^2}{2\beta}<0.$$

Thus, the striped pattern realizes the equilibrium state for $\varepsilon>0$ (or $K_b<0$). It is remarkable, that the profiles in Fig. 16 are rather straight, as in the experimental images. With three unknown parameters it is possible to fit the observed stripe

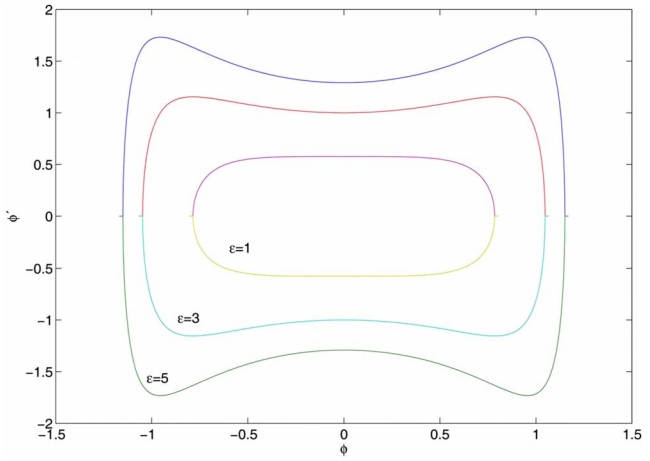

FIG. 15. (Color online) Dependence of $\varphi(\varphi')$ defined by Eq. (8).

distances as well as the stripe profiles satisfactorily. The ratio $K_{b4}/K_s=R_0^2$ essentially determines the stripe width, while K_s/K_b defines the maximum angle. This simple model is able to capture the main features of the observed pattern at least qualitatively.

The images of the striped pattern show that the period of the stripes varies considerably in a film of a constant thickness at a constant temperature. Any actual texture that has been formed in the course of propagation and folding of strings cannot simply adjust its periodicity to the energy minimum. Frustrated solutions with larger periodicities may be long-term persistent and changing of the period would require nucleation of new stripes. The transition into the equilibrium state (with a new period) can be limited by kinetics, and the system remains in a number of metastable states, leaving the stripes under dilative strain. This may explain why one often observes a coexistence of stripes of different width in the film. Since the director field is anchored at dislocations, strings cannot cross layer steps in the film. Thus frustrated patterns with different stripe distances are found in regions of different film thicknesses. In a one-

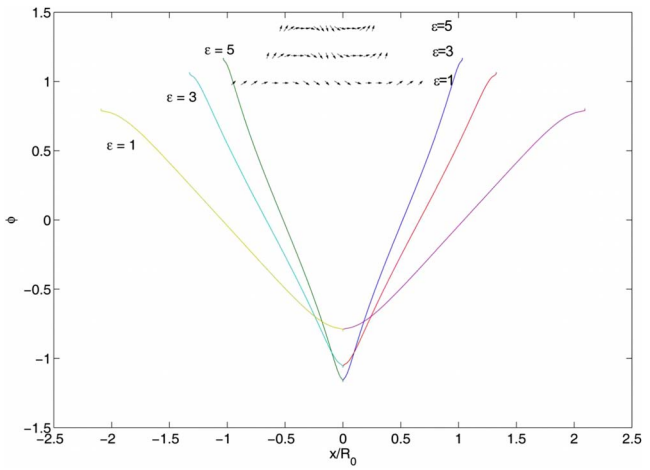

FIG. 16. (Color online) Solution $\varphi(x)$ (one period) of Eq. (8) for selected ε.

dimensional model, the insertion of regions of constant director deflection at the positions of the maxima or minima of the stripe pattern profile yields new equilibrium state, since in the absence of director gradients all torques disappear [Eq. (4)]. The modified profile is continuous everywhere, and so are the derivatives of **c**. There is no possibility for the structure to remove the constant c director plateaus in the 1D model; one may only shift and redistribute the stripes without gain of free energy. In 2D, the penetration of hairpins into the pattern can reduce the stripe distance, as found in the experiment.

What are the physical grounds for the bend elastic constant to be negative? As known from literature several physical reasons could contribute to the reduction of the effective bend elastic constant. First, the natural tendency of bent-shaped mesogens to sterically induce local bend of the nematic director can result in negative bend elastic constant as proposed by Dozov [24]. In the Landau-type model of the nematic phase formed by bent-shaped mesogens discussed in [24] a uniform director field becomes unstable, and a transition into distorted states either oscillating splay-bend or conical twist bend helix has been predicted. It has been shown experimentally that the bend elastic constant considerably decreases (by seven times) in mixtures of calamitic nematogens with bent-core molecules of increasing concentration of the latter [25]. On the other hand, in smectic phases of bent-core mesogens, sterical interactions can lead to formation of spontaneous bend of the c director (splay of p) in a PM-Sm-*CP* phase [26]. In this case only one particular sign of bend is favorable and the stripes of director bend are separated by defect walls, which is different from the behavior we observe in our compound.

Another effect specific to bent-shaped mesogens can be expected if the coupling between the *c* and *p* directors is taken into account. In contrast to the chiral Sm-C^* phase, polarization in polar banana phases, e.g., Sm-*CP*, can be independent of the molecular tilt. This gives rise to a polar biaxial Sm-*AP* phase and a Sm-*C*-Sm-*CP* transition [27,28]. Then, the coupling terms between **c** and **p** should be taken into account. It is remarkable that these directors have different symmetries: For a given $\hat{\mathbf{c}}=(c_x c_y)$ the 180° rotation of the film about the $\hat{\mathbf{x}}$ axis will transform $\hat{\mathbf{c}}$ to $\hat{\mathbf{c}}'$ so that $c_x'=-c_x(x,-y)$ and $c_y'=c_y(x,-y)$ (with the term 180° rotation we mean physically that we transform y to $-y$ and z to $-z$, redefine the layer normal **k** to **−k**, and director **n** to **−n**). On the other hand, for the *p* director $p_x'=p_x(x,-y)$ and $p_y'=-p_y(x,-y)$. Thus the product $(\nabla\times\hat{\mathbf{c}})(\nabla\cdot\mathbf{p})$ is invariant under rotations. This term is also pseudoscalar and requires a pseudoscalar elastic constant κ with handedness defined by the mutual orientations of $\hat{\mathbf{c}}$ and **p** (structural chirality in the Sm-*CP* phase). Assuming that the *c* and *p* directors are nearly orthogonal, in a given co-ordinate frame this term would contribute to the free energy as $f_{cp}=\kappa(\nabla\times\hat{\mathbf{c}})(\nabla\cdot\mathbf{p})=\kappa(\nabla\times\hat{\mathbf{c}})^2$. This means that for a given handedness, f_{cp} would reduce the effective bend elastic constant. Despite that in the experimental patterns the alternating bend deformation creates an energetically expensive polarization splay; the overall structure can be, possibly, stabilized by a flexoelectric polarization.

Chirality alone can contribute to reduction of K_b as it has been shown by Hinshaw *et al.* [22]. In their model, the au-

thors constructed the expansion of the elastic energy density in terms of the gradients of the c director accounting also for changes in the magnitude of $\mathbf{c}$:

$$f = \frac{1}{2}\{r|\mathbf{c}|^2 + u_4|\mathbf{c}|^4 + u_6|\mathbf{c}|^6\} + \frac{1}{2}[K_b|\nabla \times \mathbf{c}|^2 + K_s|\nabla \cdot \mathbf{c}|^2] + w|\mathbf{c}|^2|\nabla \times \mathbf{c}| + a_0(\nabla \times \mathbf{c}). \quad (9)$$

The terms in curly brackets come from the magnitude change of $\mathbf{c}$. The middle terms in the square brackets are the splay and bend terms. They are different from the corresponding terms in Eq. (1) since the energy is expressed in terms of the gradient of the full vector $\mathbf{c}$ and not in terms of a unit director $\hat{\mathbf{c}}$. The last two terms are chiral. The very last term can be converted into a line integral which will be accounted for in the boundary conditions. This term favors tangential anchoring of $\mathbf{c}$ in strongly chiral materials [9]. The authors in [22] have shown that Eq. (9) can be reduced to Eq. (1) for unit director with $K_s = M^2K(1+\Delta)$ and $K_b = M^2K\{(1-\Delta) - w^2/2u_4\}$, where M is a magnitude of the c director corresponding to the minimum of the free energy in the case of a uniform $\mathbf{c}$ and $u_6 \neq 0$, where $K = (K_s + K_b)$ and $\Delta = (K_s - K_b)/(K_s + K_b)$. The relation between $\mathbf{c}$ and $\hat{\mathbf{c}}$ is given by $\mathbf{c} = (M - w/4u\nabla \times \hat{\mathbf{c}})\hat{\mathbf{c}}$. It follows from the expression for K_b that the chiral coupling w reduces K_b and, when it is sufficiently strong, can make K_b negative. Thus, strong chirality of the phase favours spontaneous bend through the term proportional to a_0 and decreases K_b through the term proportional to w. Higher ordered terms are required to stabilize the striped pattern. Since the widths of the stripes with opposite bend are equal, the even power in bend terms will dominate the elastic energy.

The nature of the broken schlieren texture in thick films and droplets is unclear and requires further investigation. This texture has been observed in several different bent-shaped compounds and cannot be associated with any particular type of the phase structure. We presume that continuous bend deformations of the c director, which necessarily involve creation of spatial charge in polar materials, are electrostatically disfavored and will be hampered in thick films. Instead, domains with a homogeneous director separated by narrow defect walls become more favored and emboss the schlieren texture. This effect is thickness and temperature dependent as well. At higher temperature, where the polarization decreases, the broken schlieren texture melts into an ordinary schlieren texture.

SUMMARY

We report an unusual behavior of the polar Sm-*CP* film formed by bent-shaped mesogens. The ground state of the c director is nonuniform and represents a pattern of alternating bend deformation. Both c and p directors are continuous and the sense of local bend is independent of the chirality of the phase structure, which makes this pattern distinct from the twist-bend instability proposed by Pang *et al.* [10]. We explain this spontaneous ambidextrous bend-state by assuming that the effective bend elastic constant is negative in our film. It seems that the bent shape of the mesogens plays a crucial role in the pattern formation.

ACKNOWLEDGMENTS

The authors thank Professor Rolfe Petschek and Professor Robert Pelcovits for fruitful discussions and helpful comments. This study has been supported by Deutsche Forschungsgemeinschaft projects ER467/2-1 and STA 425/17.

[1] G. A. Hinshaw, R. G. Petschek, and R. A. Pelcovits, Phys. Rev. Lett. **60**, 1864 (1988).
[2] D. Blankschtein and R. M. Hornreich, Phys. Rev. B **32**, 3214 (1985).
[3] P. G. de Gennes and J. Prost, *The Physics of Liquid Crystals* (Clarendon Press, Oxford, 1993).
[4] F. C. Frank, Discuss. Faraday Soc. **25**, 19 (1958).
[5] C. Rosenblatt, R. B. Meyer, R. Pindak, and N. A. Clark, Phys. Rev. A **21**, 140 (1980).
[6] R. A. Pelcovits and B. I. Halperin, Phys. Rev. B **19**, 4614 (1979).
[7] J. Ruiz-Garcia, X. Qiu, M.-W. Tsao, G. Marshall, C. M. Knobler, G. A. Overbeck, and D. Mobius, J. Phys. Chem. **97**, 6955 (1993).
[8] C.-M. Chen, T. C. Lubensky, and F. C. MacKintosh, Phys. Rev. E **51**, 504 (1995).
[9] S. A. Langer and J. P. Sethna, Phys. Rev. A **34**, 5035 (1986).
[10] J. Pang and N. A. Clark, Phys. Rev. Lett. **73**, 2332 (1994).
[11] J. Maclennan and W. Seul, Phys. Rev. Lett. **69**, 2082 (1992).
[12] J. V. Selinger, Zhen-Gang Wang, R. F. Bruinsma, and Ch. M. Knobler, Phys. Rev. Lett. **70**, 1139 (1993).
[13] J. Pang, C. D. Muzny, and N. A. Clark, Phys. Rev. Lett. **69**, 2783 (1992).
[14] A. Eremin, A. Nemes, R. Stannarius, G. Pelzl, and W. Weissflog, Soft Matter **4**, 2186 (2008).
[15] J. V. Selinger, Phys. Rev. Lett. **90**, 165501 (2003).
[16] A. Eremin, S. Diele, G. Pelzl, and W. Weissflog, Phys. Rev. E **67**, 020702(R) (2003).
[17] G. Pelzl, M. W. Schröder, A. Eremin, S. Diele, B. Das, S. Grande, H. Kresse, and W. Weissflog, Eur. Phys. J. E **21**, 293 (2006).
[18] R. Amaranatha Reddy and C. Tschierske, J. Mater. Chem. **16**, 907 (2006).
[19] L. E. Hough, Ph.D. thesis, University of Colorado, Boulder, 2007.
[20] M. I. Godfrey and D. H. van Winkle, Phys. Rev. E **54**, 3752 (1996).
[21] Ch. Bohley and R. Stannarius, Soft Matter **4**, 683 (2008).
[22] G. A. Hinshaw and R. G. Petschek, Phys. Rev. A **39**, 5914 (1989).

[23] D. R. Link *et al.*, Science **278**, 1924 (1997).
[24] I. Dozov, Europhys. Lett. **56**(2), 247 (2001).
[25] B. Kundu, B. Pratibha, and N. V. Madhusudana, *Proceedings of the International Liquid Crystal Conference 2008*.
[26] D. A. Coleman, J. Fernsler, N. Chattham, M. Nakata, Y. Takanishi, E. Körblova, D. R. Link, R.-F. Shao, W. G. Jang, J. E. Maclennan, O. Mondainn-Monval, C. Boyer, W. Weissflog, G. Pelzl, L.-C. Chien, J. Zasadzinski, J. Watanabe, D. M. Walba, H. Takezoe, and N. A. Clark, Science **301**, 1204 (2003).
[27] A. Eremin, S. Diele, G. Pelzl, H. Nádasi, W. Weissflog, J. Salfetnikova, and H. Kresse, Phys. Rev. E **64**, 051707 (2001).
[28] A. Eremin, H. Nádasi, G. Pelzl, S. Diele, H. Kresse, W. Weissflog, and S. Grande, Phys. Chem. Chem. Phys. **6**, 1290 (2004).